A SIMPLE STATE-SPACE APPROACH FOR THE INVESTIGATION OF NON-NORMAL EFFECTS IN THERMOACOUSTIC SYSTEMS

Herbert Mangesius, Wolfgang Polifke*

Lehrstuhl für Thermodynamik
Technische Universität München
Boltzmannstr. 15, D-85748 Garching, Germany
* Corresponding author: polifke@tum.de

A low-order, state-space modeling approach for thermoacoustic systems has been developed, which is based on present and past values of nodal characteristic wave amplitudes. The method allows to simulate the time evolution of the system state, but also the efficient computation of the (pseudo-)spectrum of the evolution operator. It is demonstrated by comparison with a frequency-domain "network model" that eigenmodes and asymptotic linear stability are predicted correctly. The influence of various model parameters (downstream reflection coefficient, temperature ratio across the heat source, magnitude and spread of heat source time delays) on transient growth of perturbation energy is explored. Furthermore, it is shown how frequency-dependent boundary impedances can be modelled through FIR or IIR filters. The discussion in the present paper is limited to simple test cases, but the approach can be generalized to systems with non-trivial topology.

1 Introduction

The combustion dynamics community has learned in recent years that thermoacoustic systems are in general non-normal [1, 2, 10, 11]. Suijth and co-workers have investigated possible consequences of non-normality for the stability of combustion systems. In this context, a variety of comparatively simple configurations – a Rijke tube and laminar diffusion or premix flames – have been studied [1,2,10]. The models for these configurations made use of the Galerkin technique frequently used for linear and nonlinear analysis of thermoacoustic stability [3].

The motivation for the present work was to develop a modelling approach that is in a sense close to the popular low-order "network models" [4, 9, 13]. The method should be able to consider configurations with non-trivial system topology, non-ideal boundary conditions, variation of mean properties across system elements, and even realistic heat source models. At the same time, the model should result in a "standard formulation" with linear matrix operator, such that the tools developed for analysis of nonnormal effects [1, 20, 21] can be applied.

The paper is organized as follows: first the low-order "network model" for an n-τ thermoacoustic system is reviewed, as this will serve as a validation case for the new formulation. Then the state space approach is introduced, starting from a very simple application to a resonator tube, and moving on to the n-τ system. Some aspects of non-normality are then explored, in particular the impact of large and distributed time lags, and non-trivial reflection coefficients.

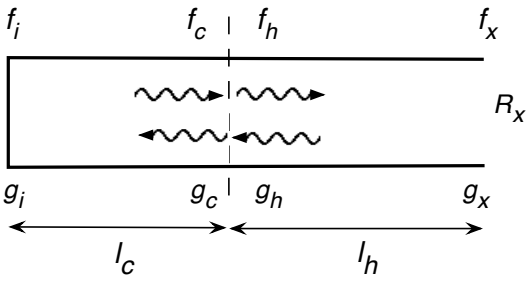

Figure 1: Network model of resonator / Rijke tube

2 Network model of n-τ-system

It is assumed that the reader is familiar with basic acoustics, so instead of starting "from scratch", we just introduce some notation and go into *medias res* quickly. We consider a system as shown in Fig. 1, i.e. a heat source placed in a duct [2, 4, 9, 13] The heat source is placed at position l_c. This parameter is not set to $l_c = L/4$, as it should be for a proper Rijke tube with two open ends, but instead considered as an adjustable model parameter.

Riemann invariants or *characteristic wave amplitudes* f and g (also denoted as p^+ and p^- by some authors) are related to the primitive acoustic variables as follows,

$$f = \frac{1}{2}\left(\frac{p'}{\rho c} + u'\right), \quad g = \frac{1}{2}\left(\frac{p'}{\rho c} - u'\right). \tag{1}$$

A downstream traveling wave f undergoes a change in phase $\exp\{i\omega l/c\}$ as it travels with the speed of sound c across the distance l_c from the inlet "i" to the cold side of the heat source "c", and similar for the wave g traveling in the upstream direction,[1]. such that the *transfer matrix* of the duct is obtained as:

$$\begin{pmatrix} f_c \\ g_c \end{pmatrix} = \begin{pmatrix} e^{-ikl_c} & 0 \\ 0 & e^{ikl_c} \end{pmatrix} \begin{pmatrix} f_i \\ g_i \end{pmatrix}. \tag{2}$$

with a wave number $k \equiv \omega/c$ for plane waves without mean flow and dissipative effects. For the duct to the right of the heat source, the transfer matrix is of the same form, but the speed of sound $c = \sqrt{\gamma RT}$ and the length l may be different.

The pressure drop across the heat source (which is a wire mesh or "gauze" in a Rijke tube) is negligible for sufficiently small mean-flow Mach numbers, $p_c = p_h$, while momentary rate of heat release $\dot{Q}(t)$ depends on the velocity $u_c(t-\tau)$ at the upstream side of the heat source "c" at an earlier time $t-\tau$. Assuming small amplitudes of perturbation and an acoustically compact heat source [4, 9, 12, 14], linearization yields the famous n-τ *model* for a heat source with time lag τ,

$$\begin{aligned} p'_h &= p'_c, \\ u'_h &= u'_c + n\,u'_c(t-\tau). \end{aligned}$$

This simple model has played a prominent role in the development of the theory of combustion instabilities in rocket engines, is used frequently as a pedagogical example, and is even relevant as a building block for models of "real-world" turbulent premix flames [2, 4, 9, 13]. The time-lag τ is an important model parameter, as it controls the phase-alignment between fluctuations of pressure and heat release and thus the sign of the Rayleigh integral. The value of τ is usually determined by convective processes and scales with the length of the heat source. The interaction index n is related to the increase in mean temperature T across the heat source. For example, $n = (T_h/T_c - 1)/2$ for the gauze of a Rijke tube. In

[1] A note on nomenclature: we make no explicit distinction between acoustic variables in the time domain and in the frequency domain. Most of the time we are in frequency space, and the f's and g's are to be understood as complex-valued Fourier transforms of time series.

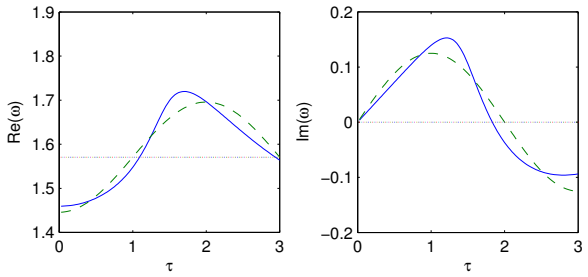

Figure 2: Frequency (left) and growth rate (right) of the fundamental mode $m = 0$ of the n-τ model with interaction index $n = 0.25$ as a function of time lag τ. Numerical solution (——) of the dispersion relation (7) vs. approximate analytical solution eq. 9) (– – –)

the present work, both n and τ are considered adjustable model parameters.

In terms of the characteristic wave amplitudes, the coupling relations across the heat source are

$$(f_h + g_h) = \xi(f_c + g_c), \quad \text{with } \xi \equiv \frac{\rho_h c_h}{\rho_c c_c}, \tag{3}$$

$$f_h - g_h = \left(1 + n\, e^{-i\omega\tau}\right)(f_c - g_c). \tag{4}$$

Without essential loss of generality, an acoustically "closed end" $u' = 0$ is imposed at the left boundary and therefore $f_i - g_i = 0$. At the right boundary, an exit reflection coefficient $R_x \equiv g_x / f_x$ may be imposed. For the moment, an "open end" with $p' = 0$ and thus $f_x + g_x = 0$ (or $R_x = -1$) is assumed.

The equations for the eight unknowns $f_i, g_i, \ldots g_x$ may be written in matrix & vector notation as

$$\mathbf{S} \begin{pmatrix} f_i \\ \vdots \\ g_x \end{pmatrix} = \begin{pmatrix} 0 \\ \vdots \\ 0 \end{pmatrix}. \tag{5}$$

with the "system matrix" $\mathbf{S}$. A non-trivial solution exists only if the *characteristic equation* $\mathrm{Det}(\mathbf{S}) = 0$ is fulfilled. Inspection of the coupling relations (2) - (4) shows, that the coefficients of the system matrix depend on geometrical and physical parameters – length l, speed of sound c, density ρ, the interaction index n, and the time lag τ – which are fixed for a given system. However, the frequency ω, which appears in the wave number and the time-lag term, is not fixed a priori. Thus, there may be *eigenfrequencies* ω_m of the system, such that $\mathrm{Det}(\mathbf{S})|_{\omega=\omega_m} = 0$.

From the characteristic equation, the *dispersion relation*

$$\cos k_c l_c \cos k_h l_h - \xi \sin k_c l_c \sin k_h l_h \left(1 + n\, e^{-i\omega\tau}\right) = 0, \tag{6}$$

can be derived [9], with $k_i = \omega / c_i; i = h, c$. This equation cannot be solved explicitly for eigenfrequencies ω_m, so in general one has to resort to numerical root finding to identify solutions.

An approximate analytical solution for the special case $l_c = l_h = l \equiv L/2$, $\rho_h = \rho_c$ and $c_c = c_h = c$ is presented in McManus et al. [9]: Introducing dimensionless variables – with duct length L and wave passage time L/c as characteristic length and time scales, respectively – the characteristic equation (6) is simplified to

$$\cos\omega - n\, e^{-i\omega\tau} \sin^2 \frac{\omega}{2} = 0. \tag{7}$$

For $n = 0$, i.e. in the absence of thermo-acoustic coupling between velocity and heat release at the gauze, the solutions to this equation are the familiar *quarter-wave* modes with wave lengths $\lambda = 1/4, 3/4, \ldots$

and frequencies

$$\omega_m = (2m+1)\frac{\pi}{2};\ m = 0,1,2,\ldots . \tag{8}$$

Note that these eigenfrequencies are purely real, so with an assumed time dependence $\sim \exp(i\omega t)$, there is no amplification or damping of the eigenmodes.

For non-zero, but small interaction index n, the eigenfrequencies can be determined approximately as $\omega_m + \omega'_m$ with small deviations $\omega'_m \ll \omega_m$ from the quarter-wave eigenfrequencies ω_m. To first order in n, ω'_m, series expansion of (7) yields

$$\omega'_m \approx (-1)^m \frac{n}{2} e^{-i\omega_m \tau}. \tag{9}$$

As explained above, an eigenmode is stable if its imaginary part

$$\Im(\omega'_m) \approx (-1)^{m+1} \frac{n}{2} \sin\omega_m \tau, \tag{10}$$

is positive, because then its amplitude decays as $\exp\left(-\Im(\omega'_m)\, t\right)$.

It is not difficult to solve the dispersion relation numerically for larger values of n (and indeed for arbitrary values of the parameters l, c, n, τ as well as arbitrary reflection coefficients at the duct ends). A simple Matlab script is included on the *n3l* CD. Numerical results for the case $n = 0.25$ are compared against the "weak interaction approximation" $n \ll 1$ in Fig. 2.

3 State-space model

Schuermans et al [15,16] have developed a powerful state space approach for thermo-acoustic systems, that is based on a modal expansion for the Green's function. For complex geometries, the basis modes for the expansion can be determined numerically (e.g. with finite-element methods), thus the method is very flexible and can be used for geometries of applied interest. The motivation for the present approach was to develop a simpler "toy model", suitable for exploring aspects of non-normality in thermo-acoustic instability.

3.1 Acoustic eigenmodes of a resonator tube

Consider an ideal resonator tube of length L with two closed ends, $u'(x=0) = u'(x=L) = 0$ as shown in Fig. 3. A discrete-time, state-space model of this system can be constructed by tracking the temporal evolution of the right-going characteristic wave amplitude f at some location "x". A state vector $\left(f^{(t)}_{x,m}\right), m = 1,\ldots M$ is introduced, with a "memory index" m such that $f^{(t)}_{x,0}$ denotes the value of the wave amplitude f_x at the present time t, while $f^{(t)}_{x,m}$ refers to an earlier time $t - m\Delta t$.

To start with the simplest possible case, a very short state vector of length $M = 2$ and a large (non-dimensional) time increment $\Delta t = 1$ are chosen. With this choice, the time increment Δt is equal to

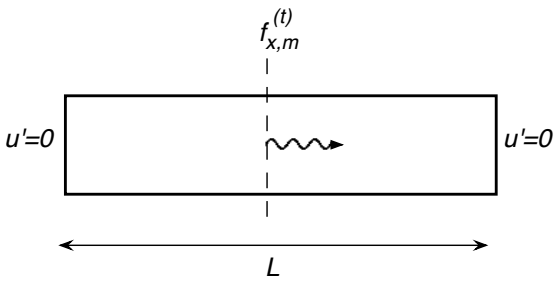

Figure 3: Wave amplitude f_x in a resonator tube of length L with two closed ends.

the time required for an acoustic wave to travel across the length of the tube. Assuming ideal reflection coefficients $R = 1$ at the closed ends and neglecting dissipation within the tube, the signal strength $|f|$ is not diminished with time.

An evolution operator for the state vector $\left(f_{x,1}^{(t)}, f_{x,2}^{(t)}\right)$ can be constructed from the following two relations:

$$f_{x,0}^{(t+1)} = f_{x,1}^{(t)}, \tag{11}$$

$$f_{x,1}^{(t+1)} = f_{x,0}^{(t)}. \tag{12}$$

The first equation expresses the fact that an acoustic signal f requires a time interval $2\Delta t = 2$ to travel once around the resonator tube. The second equation does not describe "system physics", i.e. acoustic wave propagation, but simply expresses the fact that "tomorrow's yesterday is today".

Eqns (11) and (12) allow to formulate a state-space model in standard form with evolution operator matrix $\mathbf{L}$:

$$\begin{pmatrix} f_{x,0} \\ f_{x,1} \end{pmatrix}^{(t+1)} = \mathbf{L} \begin{pmatrix} f_{x,0} \\ f_{x,1} \end{pmatrix}^{(t)} = \begin{pmatrix} 0 & 1 \\ 1 & 0 \end{pmatrix} \begin{pmatrix} f_{x,0} \\ f_{x,1} \end{pmatrix}^{(t)}. \tag{13}$$

The eigenvalues λ_i and corresponding eigenvectors $\mathbf{v}_i$, $i = 1,2$ of the matrix $\mathbf{L}$ are

$$\lambda_1 = -1,\ \mathbf{v}_1 = \begin{pmatrix} 1 \\ -1 \end{pmatrix}, \quad \lambda_2 = 1,\ \mathbf{v}_2 = \begin{pmatrix} 1 \\ 1 \end{pmatrix} \tag{14}$$

For the first eigenvector, $\mathbf{L}^2\mathbf{v}_1 = \mathbf{v}_1$, i.e. the system returns to its initial state after two time steps. In other words, the period of oscillation $T = 2\Delta t = 2$, which indicates that this eigenmodes is the well-known half-wave fundamental acoustic mode of a resonator with two closed ends. The eigenfrequency $\omega_1 = 2\pi/T = \pi$ of this mode can be deduced also directly from the eigenvalue $\lambda_1 = -1 = e^{i\pi}$: the phase advance per time step $\omega_1 \Delta t = \pi$ and therefore

$$\omega_1 = \frac{\pi}{\Delta t} = \pi,$$

which obviously corresponds to the fundamental acoustic eigenmode.

The second eigenmode found is a spurious (or "aliased") mode, because its eigenfrequency $\omega_2 = 2\pi/\Delta t$ is twice the Nyquist frequency $\omega_{\mathrm{Nyq}} = \pi/\Delta t$. In order to increase the frequency resolution and thus describe more than just the fundamental mode, it is necessary to decrease the sampling interval Δt. For example $\Delta t = 1/2$ results in a 4×4 evolution operator

$$\begin{pmatrix} f_{x,0} \\ f_{x,1} \\ f_{x,2} \\ f_{x,3} \end{pmatrix}^{(t+1)} = \begin{pmatrix} 0 & 0 & 0 & 1 \\ 1 & 0 & 0 & 0 \\ 0 & 1 & 0 & 0 \\ 0 & 0 & 1 & 0 \end{pmatrix} \begin{pmatrix} f_{x,0} \\ f_{x,1} \\ f_{x,2} \\ f_{x,3} \end{pmatrix}^{(t)}. \tag{15}$$

As in eqn (13), the first row of $\mathbf{L}$ describes wave propagation around the duct, while rows 2 – 4 merely "update history". With double the frequency resolution, we find four eigenvectors. Only the first two are physical

$$\lambda_1 = i = e^{i\pi/2},\ \mathbf{v}_1 = \begin{pmatrix} 1 \\ -i \\ -1 \\ i \end{pmatrix}, \quad \lambda_2 = -1 = e^{i\pi},\ \mathbf{v}_2 = \begin{pmatrix} 1 \\ -1 \\ 1 \\ -1 \end{pmatrix}. \tag{16}$$

The evolution operator $\mathbf{L}$ phase advances the first eigenvector $\mathbf{v}_1$ by $\pi/2$, such that four times steps are required to return to the initial state. The corresponding eigenfrequency is $\omega_1 = 2\pi/T = 2\pi/4\Delta t = \pi$, which again corresponds to the fundamental mode. The eigenfrequency of the 2nd eigenvector is twice as high, corresponding obviously to the 2nd acoustic mode with wave length equal to the length of the duct.

3.2 A state-space "network model" for the resonator tube

The simple model for a resonator tube introduced in the previous section makes use of a state vector with "memory", which is constructed from a single variable, i.e. the right-going wave f_x at one monitor point within the resonator. Now it will be shown how this formulation can be generalized to a low-order state-space model for acoustic "networks" with – in principle – arbitrary topology. With reference to fig 1, the model variables are the characteristic wave amplitudes f, g at a network "node". For the case of a resonator tube (without heat source), the node is only a monitor point, where acoustic waves pass back and forth without any scattering, such that

$$f_h = f_c \text{ and } g_c = g_h. \tag{17}$$

Wave propagation and reflection, on the other hand, imply that

$$f_{c,0}^{(t+1)} = g_{c,C}^{(t)} \qquad \text{for } (C+1)\Delta t = \tau_c = 2l_c/c_c, \tag{18}$$

$$g_{h,0}^{(t+1)} = R_x f_{h,H}^{(t)} \qquad \text{for } (H+1)\Delta t = \tau_h = 2l_h/c_h. \tag{19}$$

The parameters τ_c and τ_h denote the time lags associated with wave propagation back and forth across the upstream (index "c") and downstream ("h") sections of the setup, respectively.

From eqns (17) – (19), a state space model can be constructed in terms of the "outgoing" characteristic wave amplitudes $\left(f_{h,m}^{(t)}\right), m = 0,\dots H$ and $\left(g_{c,m}^{(t)}\right), m = 0,\dots C$. In the simplest case with $l_c/c_c = l_h/c_h$, exit reflection coefficient $R_x = 1$, and $C = H = 1$, a model with evolution operator $\mathbf{L}$ identical to the previous example is obtained:

$$\begin{pmatrix} f_{h,0} \\ f_{h,1} \\ g_{c,0} \\ g_{c,1} \end{pmatrix}^{(t+1)} = \begin{pmatrix} 0 & 0 & 0 & 1 \\ 1 & 0 & 0 & 0 \\ 0 & 1 & 0 & 0 \\ 0 & 0 & 1 & 0 \end{pmatrix} \begin{pmatrix} f_{h,0} \\ f_{h,1} \\ g_{c,0} \\ g_{c,1} \end{pmatrix}^{(t)} . \tag{20}$$

Note that the interpretation of the matrix coefficients differs from the previous case: now the 1st as well as the 3rd row express wave propagation, while only the 2nd and 4th rows represent the "history updates". Of course, the eigenfrequencies and -modes resulting from eq. (20) are identical to the previous example.

The formulation introduced in this section allows considerable flexibility. For example, with an "open end" downstream boundary condition $R_x = -1$, the quarter-wave modes with eigenfrequencies $\omega_m = 1/2, 3/2, 5/2, \dots$ are properly identified (see the example Matlab script on the *n3l* CD). The highest eigenfrequency that can be identified must be smaller than the Nyquist frequency $\omega_{\text{Nyq}} = (C+H+2)\pi/2$. More than that, it should be obvious how the ansatz presented here can be generalized to networks with several monitor planes (or "network nodes"), with the state vector comprised of present and previous values of outgoing characteristic wave amplitudes f_i and g_j. Instead of discussing an example with such non-trivial topology, it will be shown next how an $n-\tau$ heat source model can be introduced.

3.3 A state-space model for the n-τ thermoacoustic system

The state vector is constructed in terms of the wave amplitudes f_h and g_c at the heat source (the "node" of the model). The coupling relation (3) for the pressure across the heat source implies that

$$f_{h,0}^{(t+1)} + g_{h,0}^{(t+1)} = \xi f_{c,0}^{(t+1)} + \xi g_{c,0}^{(t+1)}. \tag{21}$$

Introducing eqns (18) and (19) to eliminate the variables f_c and g_h, one obtains,

$$f_{h,0}^{(t+1)} - \xi g_{c,0}^{(t+1)} = -R_x f_{h,H}^{(t)} + \xi g_{c,C}^{(t)}. \tag{22}$$

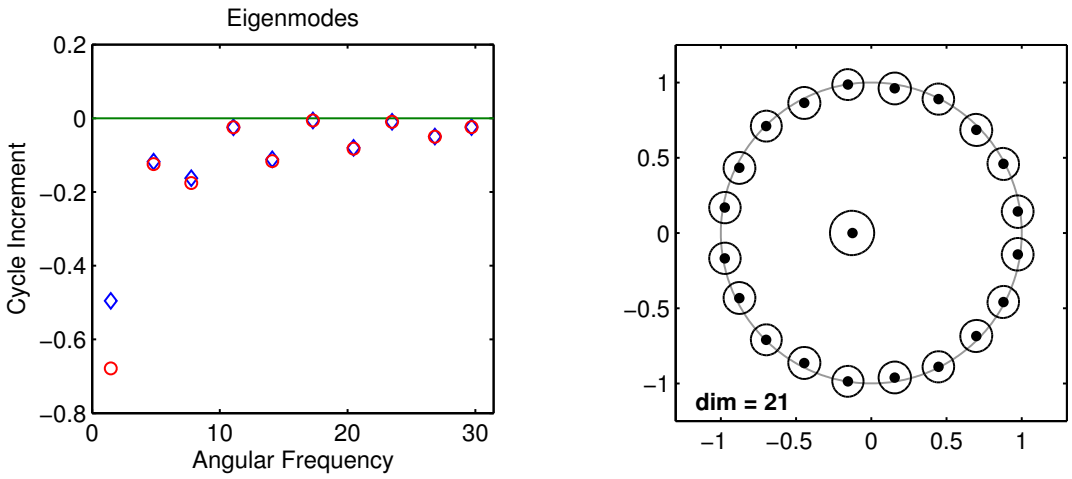

Figure 4: Spectrum and pseudospectrum of n-τ thermoacoustic system with $\tau = 0.1$, interaction index $n = 0.25$, ratio of specific impedances $\xi = 1$, and downstream reflection coefficient $R_x = -0.75$. Left: Angular frequencies (non-dimensional) and cycle increments of the first 10 eigenmodes computed from the characteristic equation of a low-order, frequency-domain model (◇) and as the eigenmodes of the operator $\mathbf{L}$ of the discrete-time, state-space model presented in this work (○). Right: Pseudospectrum of $\mathbf{L}$ for $\epsilon = 0.1$ with $C = H = 9$ and $Q = 1$

Similarly one derives from the relation (4) for the velocity fluctuations

$$f_{h,0}^{(t+1)} - g_{h,0}^{(t+1)} = f_{c,0}^{(t+1)} - g_{c,0}^{(t+1)} + n\left(f_{c,Q}^{(t+1)} - g_{c,Q}^{(t+1)}\right), \tag{23}$$

$$f_{h,0}^{(t+1)} + g_{c,0}^{(t+1)} = R_x f_{h,H}^{(t)} + g_{c,C}^{(t)} + n g_{c,C+Q}^{(t)} - n g_{c,Q-1}^{(t)}, \tag{24}$$

where $Q\Delta t = \tau$, i.e. the "memory" of the heat source extends over a number of Q time steps.

Linear combination of these two equations yields the required "state update" relations for the unknowns $f_{h,0}^{(t+1)}$ and $g_{c,0}^{(t+1)}$:

$$f_{h,0}^{(t+1)} = -R_x \frac{1-\xi}{1+\xi} f_{h,H}^{(t)} + \frac{2\xi}{1+\xi} g_{c,C}^{(t)} - \frac{n\xi}{1+\xi} g_{c,Q-1}^{(t)} + \frac{n\xi}{1+\xi} g_{c,C+Q}^{(t)}, \tag{25}$$

$$g_{c,0}^{(t+1)} = \frac{2R_x}{1+\xi} f_{h,H}^{(t)} + \frac{1-\xi}{1+\xi} g_{c,C}^{(t)} - \frac{n}{1+\xi} g_{c,Q-1}^{(t)} + \frac{n}{1+\xi} g_{c,C+Q}^{(t)}. \tag{26}$$

For the case $n = 0$ (no unsteady heat release) and $\xi = \rho_h c_h/(\rho_c c_c) = 1$ (no temperature jump, i.e. no steady heat release), these equations reduce to the relations (17) – (19) for the monitor plane of the resonator tube.

The evolution operator $\mathbf{L}$ for the n-τ system is built from these two equations plus the "history updates" for the state vector, which result in "1"-entries on the sub-diagonal.

The cycle increment Γ_m of a mode m with temporal evolution $\sim \exp(-i\omega_m t)$ is defined as the relative increment in amplitude per period of oscillation T_m,

$$\Gamma_m \equiv \exp\left(-2\pi \frac{\Im(\omega_m)}{\Re(\omega_m)}\right) - 1 \tag{27}$$

For the mth eigenmode of a discrete time model, the relative increment in amplitude per time step should be proportional to the cycle increment

$$|\lambda_m| = 1 + \frac{\Gamma_m}{T_m}\Delta t,$$

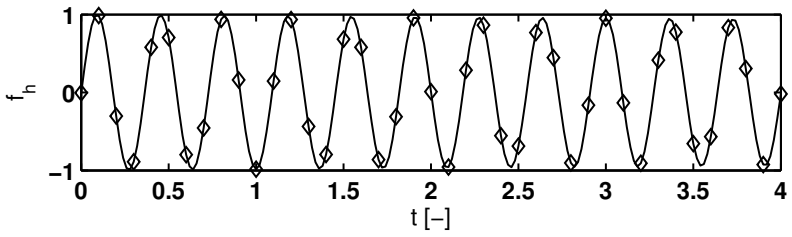

Figure 5: Time evolution of wave amplitude f_h of most unstable mode (cycle increment $\Gamma = -0.0097$) with model parameter values $\tau = 0.1$, $n = 0.25$, $\xi = 1$, $R_x = -0.75$ and time step sizes $\Delta t = 0.1$ (◇) and $\Delta t = 0.02$ (——)

and therefore

$$\Gamma_m = (|\lambda_m| - 1)\frac{T_m}{\Delta t} = (|\lambda_m| - 1)\frac{2\pi}{\arg(\lambda_m)}. \tag{28}$$

Frequencies $\Re(\omega_m)$ and cycle increments Γ_m computed with the state space model are compared against results of the low-order frequency domain model in Fig. 4. Model parameters were set to time lag $\tau = 0.1$, interaction index $n = 0.25$, ratio of specific impedances $\xi = 0.4$, and downstream reflection coefficient $R_x = -0.75$, such that all eigenmodes exhibit a negative cycle increment. Overall, the agreement between the predictions of the two formulations is very good. For large decay rates, in particular for the first mode, the comparison shows discrepancies. The following explanation is offered: for large decay rates and low frequencies (large period T_m), the amplitude reached by extrapolating the slope at time $t = 0$ to time $t = T_m$ predicts a lower amplitude than an exponential decay, where the slope decreases gradually in the time interval $0 \rightarrow T_m$.

With the state space model it is of course also possible to "march in time" by repeated application of the evolution operator $\mathbf{L}$ to an initial state vector. Exemplary results are shown in Fig. 5, which shows the temporal evolution of the most unstable mode for the chosen model parameters (see the figure caption). For this mode, the cycle increment is almost zero, the decay in amplitude over ten periods is barely discernible.

The model of Sujith at al. for the n-τ thermoacoustic system [2, 10] does not take into account a jump in mean temperature with $\xi \neq 1$ across the heat source. Also, the formulation of the heat source involves a Taylor series in time lag τ and thus is limited to small values of the time lag $\tau < 0.3$. The state space formulation presented here can take these effects into account without difficulty. In particular the time lag need not be small, such that larger, more realistic values of τ can be chosen. Furthermore, a spread in time lags, as it is often observed in flame transfer functions [6, 7] can also be considered. Results for such cases will be presented in the next section.

4 Non-normal effects

The evolution operator $\mathbf{L}$ for the resonator tube with "open end" boundary conditions $R = 1$ – see eqn (15) – is a *circulant matrix* and therefore normal [5]. One can easily confirm this numerically by checking that $\mathbf{L}\mathbf{L}^\dagger - \mathbf{L}^\dagger\mathbf{L} = 0$ (within machine accuracy). Imposing non-ideal boundary conditions with reflection coefficients $|R| \neq 1$ results in general in a non-normal operator $\mathbf{L}$, as pointed out by Nicoud et al. [11].

The evolution operator for the n-τ system with coupling conditions (25) and (26) across the heat source is also found to be non-normal provided that one or several of the following conditions are met:

- reflection at the boundaries is not ideal, $|R| \neq 1$,
- the ratio of specific impedances $\xi \equiv \rho_h c_h / \rho_c c_c \neq 1$, i.e. mean temperature T and thus density ρ and speed of sound c change across the heat source,
- the interaction index n is not zero, i.e. the rate of heat release is fluctuating

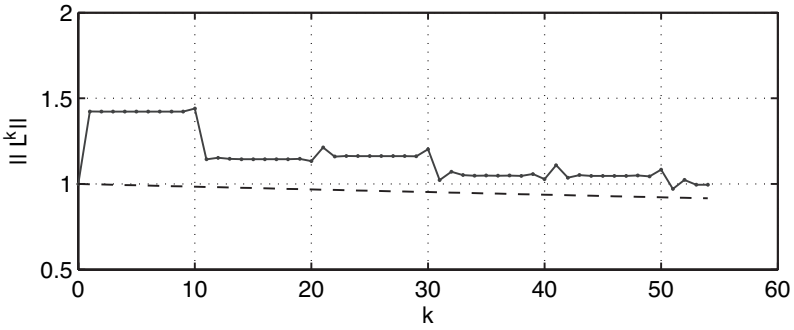

Figure 6: Transient evolution $||\mathbf{L}^k||$ for n-τ system with $\tau = 0.1$, $n = 0.25$, $\xi = 1$, $R_x = -0.75$. $C = H = 9$, such that $\Delta t = 0.1$

With the `eigtool` package of Wright [21] it is very easy to compute pseudospectra [20] of the discrete time evolution operator $\mathbf{L}$. The pseudospectrum for the linearly stable case discussed previously is shown in Fig. 4. The contour lines for $\epsilon = 0.1$ do not extend significantly beyond the unit circle, which suggests that at these conditions no strong transient growth should be expected. This is confirmed by the transient behaviour of $||\mathbf{L}^k||$ shown in Fig. 6: with the first time step, the norm jumps to a value $||\mathbf{L}^k|| \approx 1.4$, stays at that level for about 10 time steps and then decays in an erratic manner, so that $G_{\max} \approx 2$.

A ratio of specific impedances $\xi = 0.4$ corresponds to a temperature ratio $T_h/T_c = 6.25$, which is a typical value for lean combustion of hydrocarbon fuels. Changing ξ to this value results (with $C = 19, H = 9, Q = 1$) in a cycle increment $\Gamma = -0.0097$, i.e. the system is marginally linearly stable. The pseudospectrum (not shown) is very similar to the one shown in Fig. 4. The temporal evolution of the norm $||\mathbf{L}^k||$ reaches a plateau slightly above 1.5 – corresponding to $G_{\max} \approx 2$ – for time steps $k = 10$ to 20, after which decay begins.

The time lag of premix flames is often of the order $\tau \approx 0.5 - 2$ (in non-dimensional units), see e.g. [7]. Increasing the time lag to $\tau = 0.5$ only moderate transient growth with $G_{\max} \approx 2$ is observed (see e.g. the red line in Fig. 9). However, for these parameter values, even the most unstable mode decays rather quickly, while Nagaraja et al. observed that largest transient growth is often observed at the border of linear instability [10]. Thus the interaction index was increased from $n = 0.25$ to $n = 1.2$, resulting in a marginally stable system. For these conditions, persisting transient dynamics with $G_{\max} > 30$ is observed, see Fig. 7.

Finally, a heat source with a spread of time lags,

$$u'_h = u'_c + \sum_k h_k u'_c(t - k\Delta t), \tag{29}$$

was considered. A very simple configuration with $h_k = n; k = 10, 11, 12$ and $h_k = -n; k = 13, 14$. The low-frequency limit of this transfer function is the same as for the n-τ model, but an intermediate peak

R_x	-1	-0.75	-1	-0.75	-0.75	-0.75	-0.75
ξ	1	1	0.4	0.4	1	0.4	0.4
n	0	0	0	0	0.25	0.25	1.2
$\mathscr{H}(\mathbf{L})$	0	0.44	0.56	0.43	0.80	0.56	0.70
$\kappa_2(\mathbf{L})$	0	1.33	2.30	1.79	16.4	13.5	4.95

Table 1: Scalar measures of non-normality for the n-τ system with $C = 19, H = 9, Q = 10$. Lengths and times have been non-dimensionalized with l_c and $2l_c/c_c$ such that $\Delta t = 1/(C+1)$

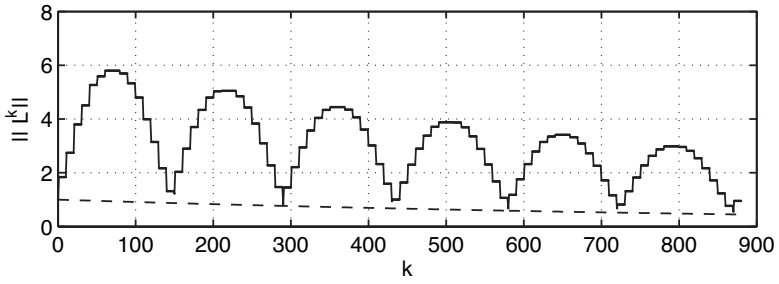

Figure 7: Transient evolution $||\mathbf{L}^k||$ for n-τ system with $\tau = 0.5$, $n = 1.2$, $\xi = 0.4$, $R_x = -0.75$. $C = 19$, such that $\Delta t = 0.05$, $H = 9$

and subsequent decay of the gain are observed, as it is typical for premix flames [6, 7, 17]. With a large interaction index $n = 1.2$, the system with distributed time lags is linearly unstable at intermediate frequencies. If one reduces n until linear stability is regained, only moderate transient growth with $G \approx 7$ after about 40 time steps is observed (not shown).

Scalar measures of non-normality [19] are the Henrici number $\mathscr{H}(\mathbf{L}) \equiv |\mathbf{L}\mathbf{L}^\dagger - \mathbf{L}^\dagger\mathbf{L}|/|\mathbf{L}|^2$ and the condition number $\kappa_2(\mathbf{L}) \equiv ||\mathbf{L}||\,||\mathbf{L}^{-1}||$. A few example values are shown in Table 1.

5 Filter based models for non-trivial transfer functions

To go beyond "toy models" with the state space ansatz presented here, it should be possible to integrate FIR or IIR filter models of acoustic elements from frequency-dependent transfer matrix coefficients (which in turn may be deduced from flame transfer functions, boundary impedances, etc). Some first results for transient evolution obtained with IIR/FIR-based models for the downstream boundary are presented in this section.

In qualitative analogy to Levine-Schwinger [8], a digital filter representing a frequency-dependent reflection of acoustic waves

$$R_x(\omega) = 1 - \frac{\omega}{\omega_{\mathrm{Nyq}}} \tag{30}$$

at the right ext "x" of the duct is adopted, see Fig. 8. The transfer function is of the form

$$H(z^{-1}) = \frac{B(z^{-1})}{A(z^{-1})} = \frac{b_0 + b_1 z^{-1} + \cdots + b_m z^{-m}}{a_0 + a_1 z^{-1} + \cdots + a_n z^{-n}}, \tag{31}$$

where z^{-1} is the shift operator, so that the k-th output can be written as weighted sum of past inputs (x) and outputs (y):

$$y(i) = \frac{1}{a_0}\left(b_0 x(i) + b_1 x(i-1) + \cdots + b_m x(i-m) - a_1 y(i-1) - \cdots a_n y(i-n)\right) \tag{32}$$

IIR and FIR filters can be distinguished, where for the latter one the output is calculated just by the inputs, thus the coefficients $a_1, \cdots, a_n = 0$ and $a_0 = 1$. IIR filters additionally maie use of past outputs (feedback) so that the same transfer function can be represented by an IIR filter of an order much smaller than the one of an adequate FIR filter. However, the use of feedback may render the overall system more unstable [18].

To implement the filter into the state-space model, the Toeplitz matrix representation for arbitrary

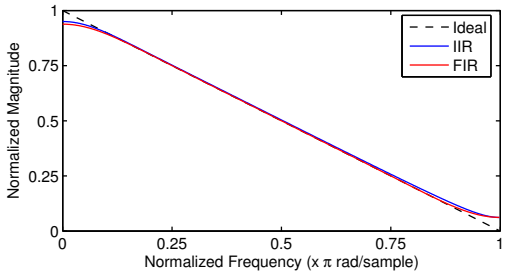

Figure 8: Transfer functions for the open end reflection: order-3 IIR filter, order-18 FIR filter and desired relation (ideal)

LTI filters is used. An output $y(i)$ is produced via the transfer function H on excitation with $x(i)$ so that

$$y = \begin{pmatrix} y(0) \\ y(1) \\ y(2) \\ \vdots \end{pmatrix} = \begin{pmatrix} h(0) & & & \\ h(1) & h(0) & & \\ h(2) & h(1) & h(0) & \\ \vdots & \ddots & \ddots & \ddots \end{pmatrix} \begin{pmatrix} x(0) \\ x(1) \\ x(2) \\ \vdots \end{pmatrix} = Hx. \tag{33}$$

This is the matrix form for the convolution operation $y(i) = h(i) * x(i) = \sum_{k=0}^{i} h_k x(i-k), \quad i = 0, 1, \ldots$ for the time discrete sampled signal. For the IIR-case the filter matrix is of size 4×4 in contrast to a 19×19 FIR filter matrix.

In Fig. 9 the transient behavior of the evolution operator including the open end reflection condition modeled by FIR and IIR filters is compared against results obtained with a constant reflection coefficient $R_x = -0.75$. With the digital filters used, discrete "jumps" in the transient evolution are less pronounced. This is not surprising, considering that the reflection coefficient imposed represents a (mild) low-pass filter. On the other hand, the filters also introduce more oscillatory or "wavy" behaviour, and $G_{\max}$ is increased. Moreover, the two filters show significant differences among each other, although their frequency response (important for long-time asymptotic behaviour) is very similar, except for the highest and lowest frequencies, see Fig. 8. The IIR filter results in a more complicated evolution, possibly due to internal dynamics caused by the feedback coefficients. Another noteworthy observation, with consequences not understood at time of writing, is that the condition number of the evolution operator $\mathbf{L}$ increases form order 10^1 to 10^{16} with introduction of the filters. This might be an indicator of pseudo-resonance.

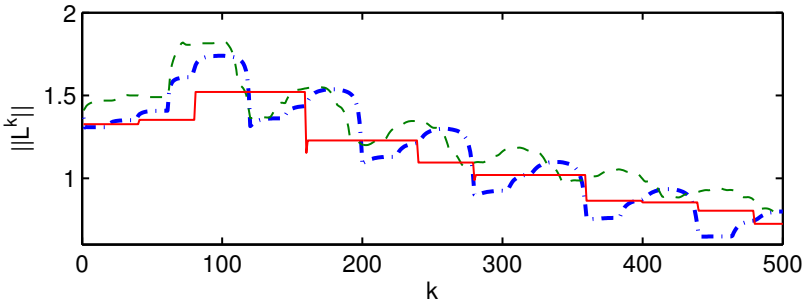

Figure 9: Transient behavior of the evolution operator with downstream reflection coefficient $R_x = -0.75$ (——), and linearly decreasing reflection coefficient described by order-3 IIR (–·–·) and order-18 FIR (– – –). Model parameters $\tau = 0.5$, $n = 0.25$, $\xi = 0.4$ $C = 79$, such that $\Delta t = 0.0125$, $H = 40$

6 Conclusions

A simple, discrete-time, state-space model for thermo-acoustic systems has been introduced[2]. Heat source models with large time lags or a spread of time lags can be considered without difficulty. Also, a jump of mean temperature, density and speed of sound across the heat source, as well as non-ideal boundary conditions with reflection coefficients $|R| \neq 1$ can be taken into account. From the evolution operator $\mathbf{L}$ for the state vector, the spectrum as well as the pseudospectrum can be computed very easily. It has been shown that results - in particular frequencies and cycle increments of eigenmodes up to the Nyquist frequency - are equivalent to predictions obtained with a standard frequency-domain, low-order "network model".

Non-ideal boundary conditions, discontinuities in specific impedance, or unsteady heat release render the evolution operator nonnormal. The pseudospectra as well as the transient evolution of $||\mathbf{L}^k||$ suggest that transient growth of oscillation energy for this model is only moderate. Note however, that a systematic search for large transient growth has not yet been carried out.

IIR or FIR filters could be used to describe acoustic elements with frequency dependent transfer matrix coefficients in the context of the state space model presented here. More realistic heat release dynamics, as it is observed, e.g, in swirl flames, or heat source models with "internal dynamics" could be considered in this way. First results obtained with IIR and FIR models for a frequency dependent boundary reflection factor have shown unexpected discrepancies, that have not yet been fully analyzed at the time of writing.

7 Acknowledgements

Much inspiration for this work comes from the AIM workshops on (thermoacoustic) stability analysis (IIT Madras, January 2009 and Univ. of Cambridge, March 2009). Discussions with R. I. Sujith, Peter Schmid, Matthew Juniper and other workshop participants are much appreciated. Special thanks to Matthew for making available his "toy models", and to Sujith for generous hospitality. Financial support for travel was provided by the Deutsche Forschungsgemeinschaft (SFB TR-40)

References

[1] K. Balasubramanian and R. Sujith. Non-normality and nonlinearity in combustion–acoustic interaction in diffusion flames. *Journal of Fluid Mechanics*, 594:29–57, 2008.

[2] K. Balasubramanian and R. Sujith. Thermoacoustic instability in a Rijke tube: Non-normality and nonlinearity. *Phys. Fluids*, (20), 2008.

[3] F.E.C. Culick. *Unsteady Motions in Combustion Chambers for Propulsion Systems*. Number AC/323(AVT-039)TP/103 in RTO AGARDograph AG-AVT-039. 2006.

[4] A. P. Dowling. The calculation of thermoacoustic oscillation. *J. of Sound and Vibration*, **180**:557–581, 1995.

[5] R.M. Gray. *Toeplitz and circulant matrices: A review*. Now Pub, 2006.

[6] A. Huber and W. Polifke. Dynamics of practical premix flames, part II: Identification and interpretation of CFD data. *Int. J. of Spray and Combustion Dynamics*, 1(2):229–250, 2009.

[7] T. Komarek and W. Polifke. Impact of swirl fluctuations on the flame response of a perfectly premixed swirl burner. *J. Eng. Gas Turbines Power*, 132(6):061503, June 2010.

[8] H. Levine and J. Schwinger. On the radiation of sound from an unflanged circular pipe. *Phys. Rev.*, 73(4):383–405, 1948.

[2] The state space approach of Schuermans et al [15, 16] is perhaps more complicated, but should be equally well suited for analysis of nonnormal effects. Perhaps the most intriguing feature of the present approach is indeed its simplicity...

[9] K. R. McManus, T. Poinsot, and S. M. Candel. A review of active control of combustion instabilities. *Prog. Energy Combust. Sci.*, **19**:1–29, 1993.

[10] Sharath Nagaraja, Kushal Kedia, and R. I. Sujith. Characterizing energy growth during combustion instabilities: Singularvalues or eigenvalues? *Proc. Comb. Inst.*, 32(1):2933–2940, 2009.

[11] F. Nicoud, L. Benoit, C. Sensiau, and T. Poinsot. Acoustic modes in combustors with complex impedances and multidimensional active flames. *AIAA Journal*, 45(2):426–441, 2007.

[12] W. Polifke. Combustion instabilities. In *Advances in Aeroacoustics and Applications*, VKI LS 2004-05, Brussels, BE, March 15 - 19 2004. Von Karman Institute.

[13] W. Polifke. System modelling and stability analysis. In *Basics of Aero-Acoustics and Thermo-Acoustics*, VKI LS 2007-02, Brussels, BE, Dec 3-7 2007. Von Karman Institute.

[14] W. Polifke, A. Poncet, C. O. Paschereit, and K. Döbbeling. Reconstruction of acoustic transfer matrices by instationary computational fluid dynamics. *J. of Sound and Vibration*, 245(3):483–510, Aug. 2001.

[15] B. Schuermans. *Modeling and Control of Thermoacoustic Instabilities.* PhD thesis, École Polytechnique Fédérale de Lausanne, 2003.

[16] B. Schuermans, V. Bellucci, D. Nowak, and C. O. Paschereit. Modelling of complex thermoacoustic systems: A state-space approach. In *Ninth Int. Congress on Sound and Vibration, ICSV9*, Orlando, FL, U.S.A., May 2002. IIAV.

[17] T. Schuller, D. Durox, and S. Candel. A unified model for the prediction of laminar flame transfer functions: Comparisons between conical and V-flame dynamics. *Combust. and Flame*, 134(1,2):21–34, 2003.

[18] J.O. Smith. Introduction to digital filters. *Center for Computer Research in Music and Acoustics (CCRMA), Stanford University*, 9, 2005.

[19] Lloyd N. Trefethen. Computation of pseudospectra. *Acta Numerica*, pages 247–295, 1999.

[20] L.N. Trefethen and M. Embree. *Spectra and pseudospectra: the behavior of nonnormal matrices and operators.* Princeton University Press, 2005.

[21] Thomas G. Wright. Eigtool. Technical report, Oxford University, 2002.